

Is CrO₂ Fully Spin Polarized? Analysis of Andreev Spectra and Excess Current

Tomas Löfwander,¹ Roland Grein,² and Matthias Eschrig^{2,3}

¹Department of Microtechnology and Nanoscience—MC2, Chalmers University of Technology, SE-412 96 Göteborg, Sweden

²Institut für Theoretische Festkörperphysik and DFG-Center for Functional Nanostructures, Karlsruhe Institute of Technology, D-76128 Karlsruhe, Germany

³Fachbereich Physik, Universität Konstanz, D-78457 Konstanz, Germany

(Received 19 July 2010; published 10 November 2010)

We report an extensive theoretical analysis of point-contact Andreev reflection data available in the literature on ferromagnetic CrO₂. We find that the spectra can be well understood within a model of fully spin-polarized bands in CrO₂ together with spin-active scattering at the contact. This is in contrast to analysis of the data within extended Blonder-Tinkham-Klapwijk models, which lead to a spin polarization varying between 50% and 100% depending on the transparency of the interface. We propose to utilize both the temperature dependence of the spectra and the excess current at voltages above the gap to resolve the spin polarization in CrO₂ in a new generation of experiments.

DOI: 10.1103/PhysRevLett.105.207001

PACS numbers: 74.45.+c, 72.25.Mk, 74.50.+r, 74.55.+v

Half-metallic ferromagnets are materials with one of the two spin bands metallic and the other insulating. Their characterization has attracted great attention, since a fully spin-polarized ferromagnetic material can be very useful for fabricating spin batteries and ideal magnetic tunnel junctions used in spintronics applications [1]. There are only a few materials that are suspected half-metals [2], one of them being CrO₂.

Following early experiments by Soulen *et al.* [3] and by Upadhyay *et al.* [4], point-contact Andreev reflection (PCAR) has been extensively used to probe the spin-polarization of strong ferromagnets. In this method a nano-sized point contact is formed by pressing a superconducting tip into the ferromagnetic material. The conductance-voltage characteristics are recorded and compared with theory in order to extract the polarization of the ferromagnet. The key ingredient in these experiments is the suppression with increased spin polarization of the Andreev reflection processes. Andreev reflection is the scattering event at which an electron quasiparticle incident from a nonsuperconducting metal is retro-reflected as a hole quasiparticle in the opposite-spin band. Charge conservation is upheld by injection of a Cooper pair into the superconductor. With increased spin polarization such retroreflection is suppressed.

In recent experiments [5,6], supercurrent was observed to flow in long Josephson junctions of CrO₂. If CrO₂ is half-metallic, these observations indicate that a conversion of supercurrent carried by spin singlet Cooper pairs in the superconductors to supercurrent carried by triplet (equal spin) Cooper pairs in the half-metal is taking place. We have [7] proposed a conversion mechanism based on spin-active interface scattering. The question arises, if this model stands the test of other experiments. Here, we show that spin-active interface scattering can explain also the PCAR experiments [3,8–15] on CrO₂ within a model that assumes fully spin-polarized bands.

The conventional analysis of the PCAR experiments (see Fig. 1 for the set-up) relies upon an extended Blonder-Tinkham-Klapwijk (BTK) formula [16], consisting of two terms. The first term includes Andreev scattering and is the usual BTK formula [17] for a point contact with an unpolarized material. The second term is the conductance of a point contact with a completely spin-polarized material for which Andreev reflection is absent. The two terms are weighted according to the formula $G = (1 - P)G_N + PG_H$, where P is the transport spin polarization. Taking the limits $V \rightarrow 0$ and $T \rightarrow 0$, the conductance would reach $G(0) = 2(1 - P)G_n$ for an ideal contact without backscattering (unit transparency) since then $G_N \rightarrow 2G_n$ while $G_H = 0$ in the whole subgap range. Here, G_n is the conductance in the nonsuperconducting state. The BTK model includes an interface barrier modeled by a delta-function potential quantified by a dimensionless parameter Z , where $Z = 0$ corresponds to unit transparency and $Z \gg 1$ to low transparency. The fit of the conductance-vs-voltage data results in values for the barrier strength Z and the polarization P . It has often been necessary to also use the superconducting gap Δ as fit parameter. Since the

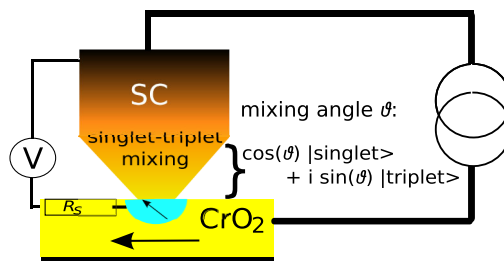


FIG. 1 (color online). Point contact between a superconductor (SC) and ferromagnetic CrO₂, including a spin-active scattering region. The arrows indicate a contact effective magnetic moment and the bulk magnetization.

gap is a fit parameter, the gap feature in the spectrum is shifted in an unpredictable way. A shifted peak position has been attributed to either a suppressed superconducting order parameter near the contact (shift to lower voltage) or a spread resistance (shift to higher voltage). The spread resistance R_s is the resistance of the material between the contact (the tip) and the voltage probe which should have been eliminated if a true four-point measurement could have been set up [14]; see Fig. 1.

It is very unsatisfactory that the existing analyses of the PCAR experiments [3,8–15] with the extended BTK formula have given a wide spectrum of spin polarizations in CrO_2 ranging from 50% to 100%. In most experiments the barrier strength is low, with a Z between 0 and 2. This sample to sample variation leads to a most likely spurious dependence of the polarization (a bulk material property) on Z (an interface property). It has been argued that the intrinsic polarization can be obtained by extrapolating the dependence $P(Z)$ to $Z = 0$ (for example Ref. [11]), although this procedure is questionable since the functional dependence $P(Z)$ is unknown [14]. The suppression of spin polarization from the expected $P = 100\%$ has in some cases been attributed to the unknown interface region. Here, we provide a model for this effect. Another unsatisfactory feature of the extended BTK model is that the gap Δ must be used as the fit parameter. Indeed, well-characterized superconducting STM tips display the bulk gap [18].

In a different experimental setup [19], Zeeman split conductance curves of CrO_2/Al junctions with fabricated tunnel barriers were measured with the Meservey-Tedrow technique [20]. The observed simple linear shift of the spectra with applied field strongly points to complete spin polarization in CrO_2 , in sharp contrast to the picture emerging from the analysis of the PCAR data with the extended BTK theory.

We give here an alternative interpretation of the PCAR experiments on CrO_2 , where we at the outset assume a spin polarization of 100% at the Fermi level and then fit the data with two interface parameters: besides Z we utilize the spin-mixing angle ϑ that describes the difference in scattering phase factors picked up by electrons of opposite spin. This spin-mixing leads to a mixture of singlet and triplet Cooper pairs in the superconductor close to the contact. If spin-flip scattering is present at the contact, triplet correlations are induced also in CrO_2 [7]. Spin flips can be induced, for example, by having misaligned moments at the contact, as depicted by the light blue contact area in Fig. 1 where the magnetization is misaligned with respect to the bulk CrO_2 [21]. When discussing PCAR, this physics is closely related to a spin-flip Andreev reflection process that leads to enhanced subgap conductance, here simply tuned by the fit-parameter ϑ . The formula for the conductance relevant for a half-metallic ferromagnet with a spin-active interface has been derived within the quasiclassical theory of superconductivity and is presented as Eqs. (153–157) in Ref. [22].

We have made a fit to all available PCAR data on CrO_2 with the spin-active interface model [23]. To make the comparison between the two scenarios consistent, we have also made new improved fits of the data to the extended BTK model of Mazin *et al.* [16], since a variety of extended BTK models have been used in the literature. The resulting fit parameters are presented in Table I and four representative data fits are shown in Fig. 2.

In Fig. 2(a) we show the data of Soulen *et al.* [3] together with the excellent fit to the spin-active interface model (red solid line). The blue dotted line is the fit to the extended BTK model without using the gap as the fit parameter. Clearly, the fit is not good. On the other hand, by letting Δ vary freely the fit can be improved except for about 10 data points in the low-voltage region (blue dashed line, Δ reduced by 33%). The overall fit, the χ^2 measure, is satisfactory in this case. In Fig. 2(b) we show the fit to a set of data from DeSisto *et al.* [8]. In this case the modified BTK fit can be made excellent by reducing Δ by 10%. Both models give satisfactory χ^2 measures, although three data points at low voltage are not perfectly fitted by the spin-active model. In Figs. 2(c) and 2(d) we show two other representative fits to both models. Again, in (d) the gap had to be reduced by about 30% to improve the fit to the modified BTK model.

From the obtained fit parameters presented in Table I, we can draw several conclusions. The main finding of this paper is that from a nonlinear curve fit (χ^2) perspective, all data sets can be fit well with the spin-active interface model with 100% spin polarization at the Fermi level of CrO_2 . This provides a complementary picture to the one emerging from the traditional extended BTK model fit. This is also reflected in the same order of magnitudes in the calculated average variances $\sigma = \chi^2/N$ (where N is the number of data points in each set) for the two models, shown in Fig. 3(d). The spin-mixing angle, here quantifying spin-flip Andreev reflection at the interface, is varying between samples but is suppressed in high- Z junctions. This is consistent with the picture of the origin of the spin-mixing effect at interfaces to strong ferromagnets [7], where the minority spin electrons gain an additional phase compared with majority spins during reflection inside the classically forbidden region in the half-metallic ferromagnet. As the barrier between the materials is enhanced, this effect is reduced.

The wide spread of the spin polarization P resulting from the extended BTK model (50% to 100%) is unsatisfactory, since P is a bulk property. We find a correlation between spin-polarization P and the barrier strength Z , see Fig. 3(a), where (as reported before) P appears to approach 100% as $Z \rightarrow 0$. We have utilized the (normalized to the contact resistance) spread resistance $r_s = R_s/R_n$ as the fit parameter in both models, although it plays a more important role for the fit with the extended BTK model. The variation of r_s with barrier strength is shown in Figs. 3(a) and 3(c). Only in one reference has the spread resistance

TABLE I. Results of nonlinear curve fits of the extended BTK model (middle set of columns) and the spin-active interface model (right set of columns) to point-contact Andreev reflection data on CrO_2 with superconducting tips of Nb ($\Delta(T=0) = 1.5$ meV, $T_c = 9.2$ K) and Pb ($\Delta(T=0) = 1.35$ meV, $T_c = 7.2$ K). We have obtained improved fits to the extended BTK model [16] by including a series resistance $r_s = R_s/R_n$ normalized to the point-contact resistance R_n as a fourth fit parameter [14]. The resulting spin polarization P , barrier strength parameter Z , and zero temperature gap parameter Δ are therefore different than found in the original papers. In the spin-active interface model the bulk quantities are fixed ($P = 100\%$ and Δ retains its bulk value), while two interface parameters (barrier strength Z and spin-mixing angle ϑ) and the series resistance r_s have been used as fit parameters. The report in Ref. [15] only contains the fit parameters, but no spectra.

# Reference	tip	T [K]	Extended BTK model						Spin-active interface model					
			P [%]	Z	Δ [meV]	r_s	χ^2		P [%]	Z	ϑ/π	Δ [meV]	r_s	χ^2
1. Soulen <i>et al.</i> [3]	Nb	1.6	66	0.90	1.0	0.05	0.34		100	0.12	0.58	1.5	0	0.32
2. DeSisto <i>et al.</i> [8]	Pb	1.7	54	1.0	1.2	0.02	0.038		100	0.28	0.44	1.35	0.05	0.065
3. Ji <i>et al.</i> [9] Fig. 4(a)	Pb	1.85	57	1.1	1.48	0	0.067		100	0.70	0.17	1.35	0.08	0.22
4. Ji <i>et al.</i> [9] Fig. 4(b)	Pb	1.85	72	0.87	1.43	0.05	0.025		100	0.38	0.22	1.35	0.17	0.091
5. Ji <i>et al.</i> [9] Fig. 4(c)	Pb	1.85	94	0.50	1.0	0.32	0.090		100	0.023	0.36	1.35	0	0.093
6. Ji <i>et al.</i> [9] Fig. 4(d)	Pb	1.85	98	0	0.9	0.42	0.062		100	0	0.39	1.35	0.06	0.087
7. Anguelouch [10] Fig. 1(a)	Pb	1.6	63	1.3	1.35	0	0.10		100	0.57	0.23	1.35	0.06	0.15
8. Anguelouch [10] Fig. 1(b)	Pb	1.6	94	0.12	1.1	0.13	0.078		100	0.26	0.28	1.35	0.02	0.081
9. Anguelouch [10] Fig. 1(c)	Pb	1.6	96	0.18	1.0	0.16	0.24		100	0.058	0.34	1.35	0	0.22
10. Anguelouch <i>et al.</i> [11]	Pb	1.6	97	0	0.94	0.29	0.27		100	0.035	0.35	1.35	0	0.28
11. Osofsky <i>et al.</i> [12]	Pb	1.7	64	1.0	1.17	0	0.19		100	0.26	0.40	1.35	0	0.21
12. Osofsky <i>et al.</i> [13]	Nb	1.7	70	1.0	1.3	0	0.21		100	0.26	0.37	1.5	0	0.20
Woods <i>et al.</i> [14]	Sn/Pb	1.75	80	0.96	0.59/1.2	0.28	...							
Yates <i>et al.</i> [15]	Pb	4.2	65–100	0–1.7	0.9–1.3							

been discussed seriously (Woods *et al.* [14]). However, because we found an uncertainty concerning their data we do not present a fit here [24]. It is crucial to use Δ as the fit parameter in the extended BTK model, while such variation does not improve the fits to the spin-active interface model. It is unclear why the (bulk) Δ should vary so

much [see Fig. 3(b)], in contrast to other experiments with superconducting STM tips [18]. All point contacts appear to be highly transparent with a small barrier strength parameter $Z < 1$. This is consistent with a Fermi velocity mismatch, which for Pb/ CrO_2 was estimated in Ref. [15] to give $Z \approx 0.26$. But this phenomenological parameter

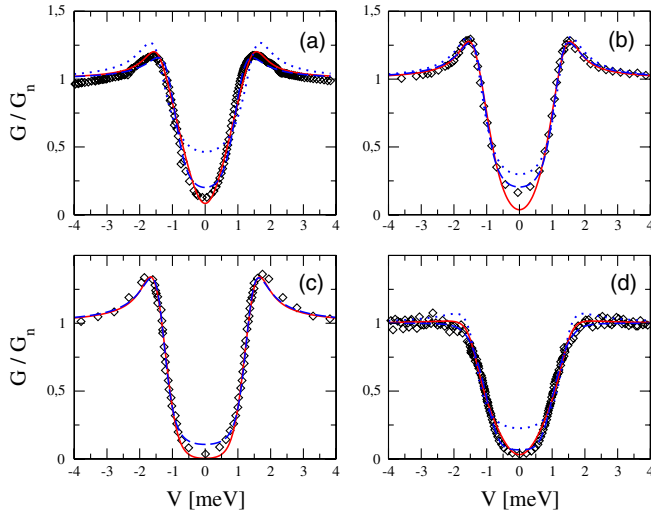


FIG. 2 (color online). Point-contact Andreev reflection data on CrO_2 from the literature and nonlinear curve-fits to the theory of superconductor-half-metallic ferromagnet point contact with spin-active interface (red solid lines) and the extended BTK model (blue dashed lines). The blue dotted lines are fits to the modified BTK model without using Δ as fit-parameter. Panels (a)-(d) are the data sets 1, 2, 7, and 10 in Table I.

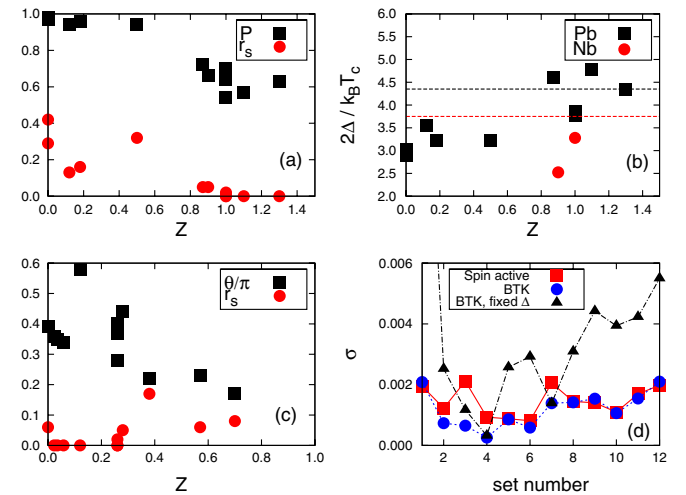


FIG. 3 (color online). Correlations between fit parameters. (a) Spin polarization P and series resistance r_s versus the barrier strength Z in the modified BTK model. (b) The superconducting gap Δ versus Z in the modified BTK model. (c) Spin-mixing angle ϑ and r_s versus Z in the spin-active interface model. (d) Comparison of the fitting function χ^2 divided by the number of data points N for the two models.

should include a range of effects causing mismatch between the materials.

We are able to fit the experimental data with three parameters describing the interface (ϑ and Z) or the geometry (r_s), while the extended BTK model relies for the same spectra on four fit parameters among which two (P and Δ) pertain to bulk properties, one to the interface (Z), and one to the geometry (r_s). The part of the spectra hardest to fit to either model is the low-voltage region. In this region there are typically much less data points than in the high voltage region [for example Figs. 2(b) and 2(c)]. This typically happens in a current bias set-up, which is not ideal for PCAR. Our fits could be further improved if we would allow for broadening in the form of a convolution with a Gaussian (as used in Ref. [15]), which would describe, e.g., voltage fluctuations. Since we do not know all experimental uncertainties we leave this question open for future experiments.

We would like to point out a few details of importance for future PCAR experiments, which may shed more light on the properties of CrO_2 . Thermal smearing is important, since it gives a considerable increase of $G(V=0)$ as compared with the $T \rightarrow 0$ limit at the temperatures used in the experiments. For the spin-active interface model, $G(0) \rightarrow 0$ as $T \rightarrow 0$ independently of the barrier strength. This is a unique feature that has not been fully explored experimentally. In our model this is a result of vanishing spectral current $j_\varepsilon = 0$ at the Fermi energy $\varepsilon = 0$. In contrast, in the extended BTK model, $G(0)$ saturates at a value given by the polarization and barrier strength; see Figs. 4(a) and 4(b). Thus, the temperature dependence of $G(0)$ in a well-defined voltage bias setup can be used as a consistency check between experiment and theory.

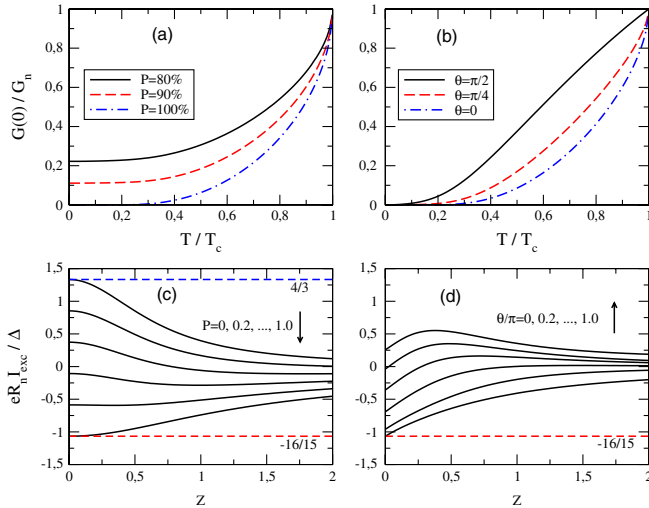


FIG. 4 (color online). Temperature dependence of the zero-voltage conductance as predicted by (a) the modified BTK model and (b) the spin-active interface model. Excess current at $V \gg \Delta/e$ versus barrier strength parameter Z as predicted by (c) the modified BTK model and (d) the spin-active interface model.

Another quantity that has not been explored experimentally so far is the excess current, formally defined as $I_{\text{exc}} = \lim_{V \rightarrow \infty} [I(V) - I_n(V)]$, where $I_n(V)$ is the current in the normal state ($= R_n V$ according to Ohm's law). In certain limits, the excess current can be computed analytically although the formulas are rather cumbersome. We present the excess currents predicted by the two models in Figs. 4(c) and 4(d). A measurement of the excess current in addition to the PCAR spectrum can be used to pin down one of the fit parameters (or as consistency check) in future experiments.

In conclusion, a number of PCAR spectra of CrO_2 have been presented in the literature where, by comparing the data to extended BTK models, a putative spin polarization between 50% and 100% has been extracted. This is in contrast to Zeeman split conductance measurements where 100% polarization was found. We have provided an alternative view of the PCAR data, where the spin polarization is 100%, but the scattering at the contact is spin active.

- [1] W. E. Pickett and J. S. Moodera, *Phys. Today* **54**, No. 5, 39 (2001).
- [2] M. I. Katsnelson *et al.*, *Rev. Mod. Phys.* **80**, 315 (2008).
- [3] R. J. Soulen, Jr. *et al.*, *Science* **282**, 85 (1998).
- [4] S. K. Upadhyay *et al.*, *Phys. Rev. Lett.* **81**, 3247 (1998).
- [5] R. S. Keizer *et al.*, *Nature (London)* **439**, 825 (2006).
- [6] M. S. Anwar *et al.*, *Phys. Rev. B* **82**, 100501(R) (2010).
- [7] M. Eschrig and T. Löfwander, *Nature Phys.* **4**, 138 (2008).
- [8] W. J. DeSisto *et al.*, *Appl. Phys. Lett.* **76**, 3789 (2000).
- [9] Y. Ji *et al.*, *Phys. Rev. Lett.* **86**, 5585 (2001).
- [10] A. Anguelouch *et al.*, *Phys. Rev. B* **64**, 180408(R) (2001).
- [11] A. Anguelouch *et al.*, *J. Appl. Phys.* **91**, 7140 (2002).
- [12] M. S. Osofsky *et al.*, *Physica (Amsterdam)* **341-348C**, 1527 (2000).
- [13] M. S. Osofsky *et al.*, *Mater. Sci. Eng. B* **84**, 49 (2001).
- [14] G. T. Woods *et al.*, *Phys. Rev. B* **70**, 054416 (2004).
- [15] K. A. Yates *et al.*, *Appl. Phys. Lett.* **91**, 172504 (2007).
- [16] I. I. Mazin, A. A. Golubov, and B. Nadgorny, *J. Appl. Phys.* **89**, 7576 (2001).
- [17] G. E. Blonder, M. Tinkham, and T. M. Klapwijk, *Phys. Rev. B* **25**, 4515 (1982).
- [18] J. G. Rodrigo, H. Suderow, and S. Vieira, *Eur. Phys. J. B* **40**, 483 (2004).
- [19] J. S. Parker *et al.*, *Phys. Rev. Lett.* **88**, 196601 (2002).
- [20] R. Meservey and P. M. Tedrow, *Phys. Rep.* **238**, 173 (1994).
- [21] Here we report results for a misalignment angle $\alpha = \pi/2$. The resulting fits are qualitatively the same for $\alpha > 0.3\pi$.
- [22] M. Eschrig, *Phys. Rev. B* **80**, 134511 (2009).
- [23] Our model includes a variation of the spin-mixing angle with impact angle θ_p in accordance with a δ -function potential of strength Z : $\vartheta(\theta_p) = \vartheta(0)\cos^2(\theta_p)$.
- [24] The data shown in Ref. [14], Fig. 4, is presented as being for a Sn/CrO₂ contact. However, using $T = 1.75$ K and $T_c^{\text{Sn}} = 3.7$ K or $T_c^{\text{Pb}} = 7.2$ K in the thermally smeared version of the formulas presented in Ref. [16] we could reproduce the curve in Fig. 4(a) of Ref. [14] only by assuming a Pb counterelectrode.